

Exploring uncertainty of trends in the lower-tropospheric North Pacific Jet position

Tom Keel¹, Chris Brierley¹, Tamsin Edwards², and Thomas Henry Alexander Frame³

¹University College London

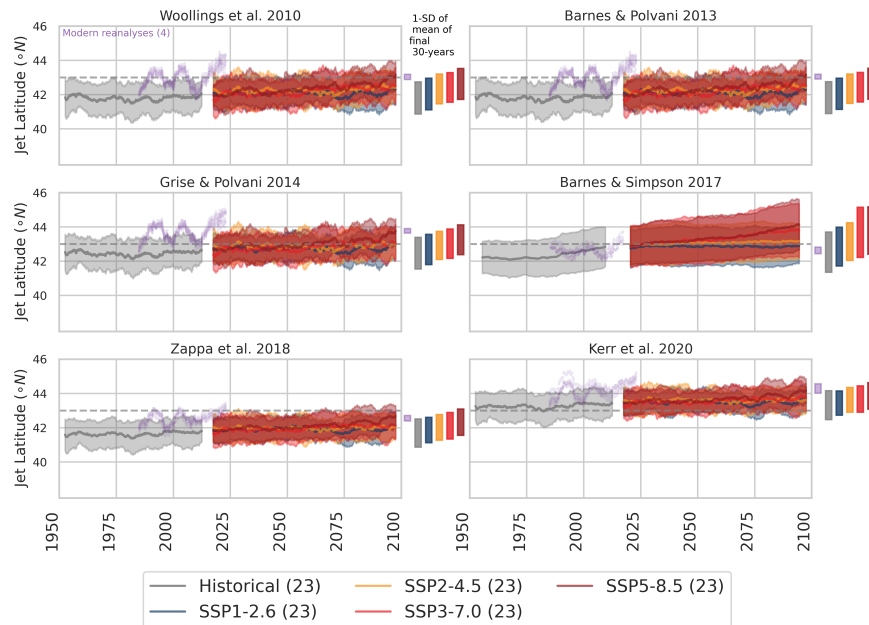
²King's College London

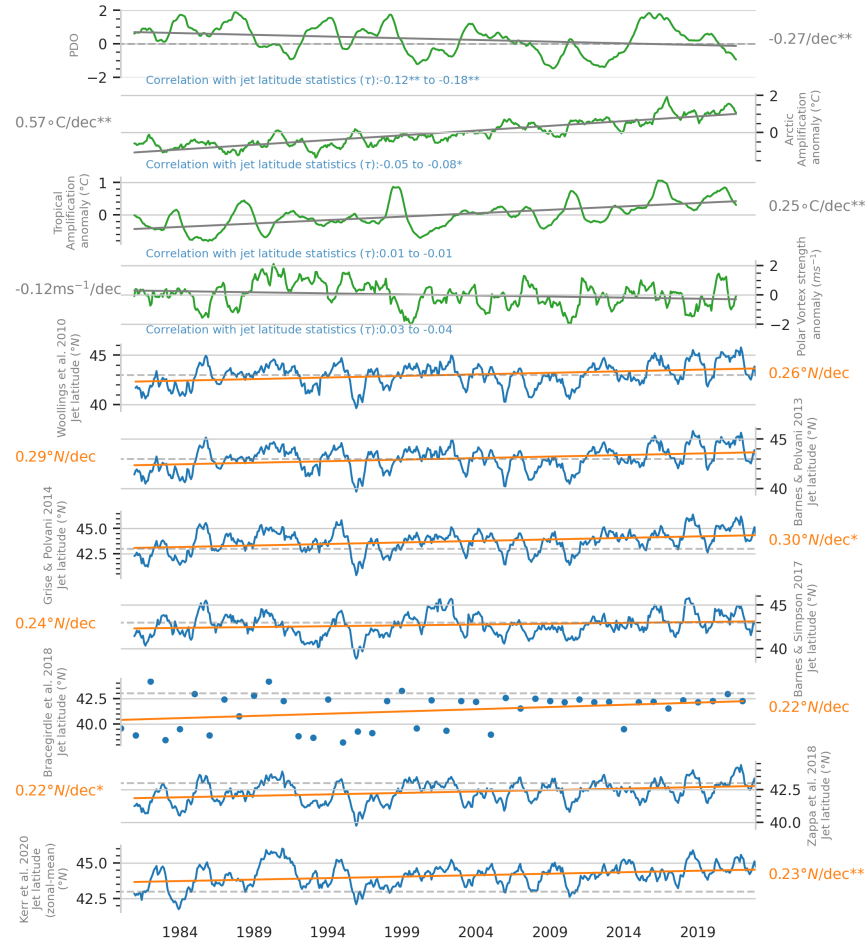
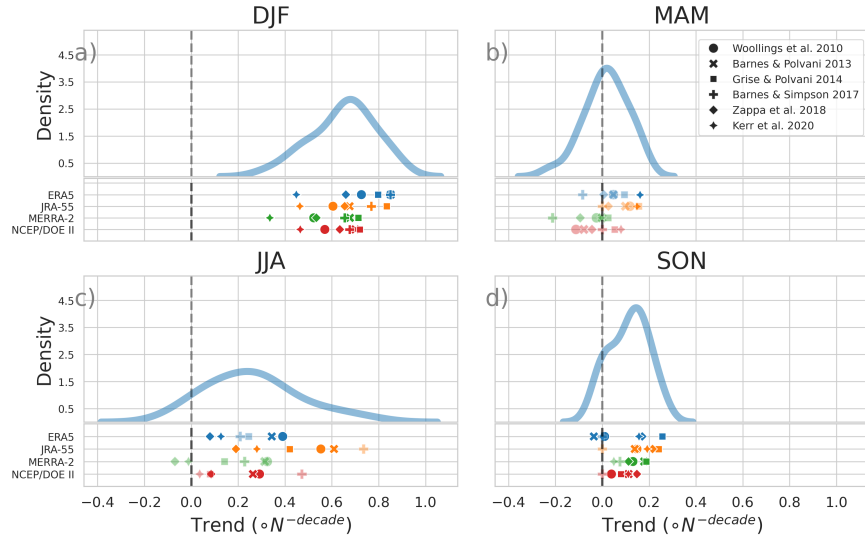
³University of Reading

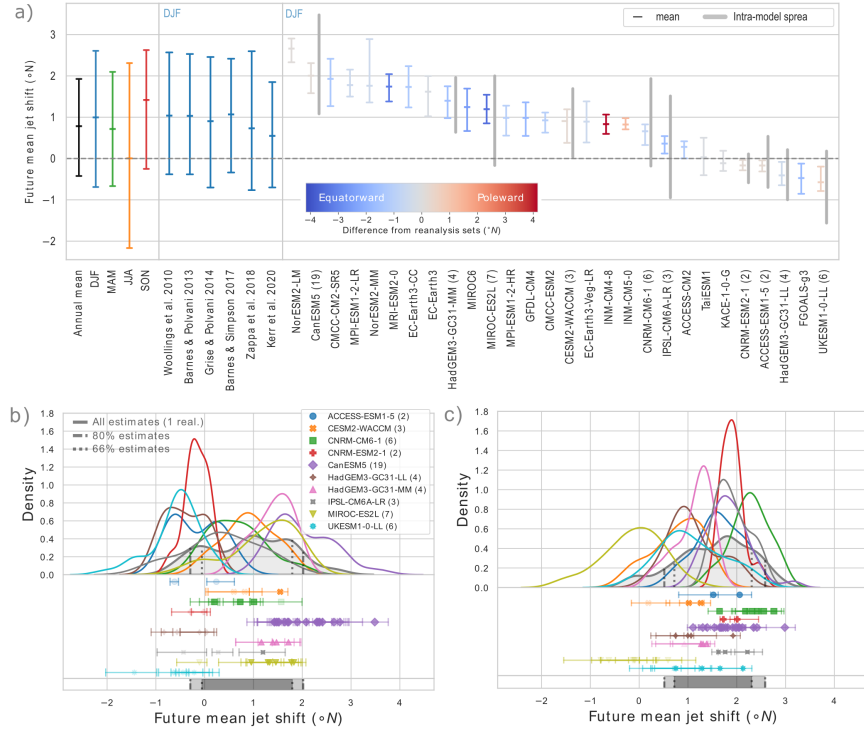
April 16, 2024

Abstract

It has been difficult to establish trends in the observed jet streams, despite modelling studies suggesting they will move polewards in a warming world. While this is partly due to biases between the models and observations, we propose that another uncertainty is rooted in the choice of statistic used to determine the ‘jet latitude’ — one measure used to quantify the jet position. We use seven different jet latitude statistics, four climate reanalysis products, and CMIP6 simulations to assess the relative importance of different uncertainties associated with North Pacific Jet (NPJ) trends. Our results show a statistically significant poleward trend in the observed winter NPJ across all reanalyses and using all jet latitude statistics. The magnitude of this trend is most sensitive to the choice of statistic. Furthermore, we find that the NPJ shifts poleward in Autumn under high emission scenarios, which is robust to the choice of jet statistic.







1 **Exploring uncertainty of trends in the**
2 **lower-tropospheric North Pacific Jet position**

3 **Tom Keel^{1,2}, Chris Brierley¹, Tamsin Edwards², and Thomas H. A. Frame³**

4 ¹Department of Geography, University College London, Gower Street, London, UK

5 ²Department of Geography, King's College London, 40 Bush House, London, UK

6 ³Department of Meteorology, University of Reading, Reading, UK

7 **Key Points:**

- 8 • We find a significant poleward trend in the winter North Pacific Jet position that
9 is robust to reanalysis and metric uncertainty.
10 • The choice of jet metric creates more uncertainty than the choice of reanalysis in
11 estimating the winter North Pacific Jet trend.
12 • We find an end-of-century poleward shift during autumn under very high emis-
13 sions that is robust to metric and model uncertainty.

Abstract

It has been difficult to establish trends in the observed jet streams, despite modelling studies suggesting that they will move polewards in a warming world. While this is partly due to biases between the models and observations, we propose that another uncertainty is rooted in the choice of statistic used to determine the ‘jet latitude’ — one measure used to quantify the jet position. We use seven different jet latitude statistics, four climate reanalysis products, and CMIP6 simulations to assess the relative importance of different uncertainties associated with North Pacific Jet (NPJ) trends. Our results show a statistically significant poleward trend in the observed winter NPJ across all reanalyses and using all jet latitude statistics. The magnitude of this trend is most sensitive to the choice of statistic. Furthermore, we find that the NPJ shifts poleward in Autumn under high emission scenarios, which is robust to the choice of jet statistic.

Plain Language Summary

Jet streams are ribbons of fast-flowing air that flow from west to east in both hemispheres high up in the atmosphere. Their speed and position affect how moisture and heat are transported across the planet, such that they act as an important control on surface weather patterns. In a warming world, the atmosphere does not warm uniformly, creating an imbalance in the processes determining where jet streams form. While climate models have generally suggested that these processes will shift the jet streams towards the poles, this has been difficult to establish in observations. Here, we argue that a major part of the uncertainty of determining this poleward trend comes from precisely which statistic is used to define a jet’s location. Our analysis measures the differences in the North Pacific Jet position trend using different jet statistics and datasets. We show that the choice of statistic used to define the jet stream produces more uncertainty than the choice of dataset. We find a statistically significant poleward trend in the wintertime North Pacific Jet position in the observational record and a significant end-of-century autumn poleward shift projected under very high emission scenarios.

1 Introduction

Jet streams are instantaneous features of the Earth’s general atmospheric circulation that manifest as fast-flowing ribbons of air and develop near the tropopause (Vallis, 2019). The impact of increased anthropogenic greenhouse gas concentrations on the climatological position of the jet streams has received much attention recently, but it has been difficult to establish trends in their position that are robust to both modelling and observational analysis (Archer & Caldeira, 2008; Cohen et al., 2020; Stendel et al., 2021). Modelling studies generally predict a poleward shift of the jet’s position in response to an amplified upper-level tropical warming, which is expected to strengthen the upper-level poleward temperature gradient in the 21st century (Lu et al., 2007; Lorenz & DeWeaver, 2007; Rivière, 2011; Santer et al., 2017). On the other hand, modelling has also shown the sensitivity of jet position to a competing effect, lower-level Arctic Amplification, which acts to mute the poleward shift of the Northern Hemisphere jets in winter (Peings et al., 2019; Curtis et al., 2020; Screen et al., 2022).

From observational research, there has generally been little consensus about the past movement of the jet position. Recently, trends have begun emerging that share similarities to trends in modelling studies: i.e. a (weak) poleward trend of the jet position in the last few decades (e.g. Martin, 2021; Woollings et al., 2023). However, these findings are subject to significant uncertainties and are not fully consistent with modelling research (Cohen et al., 2020; Oudar et al., 2020). We propose that this is partly due to the influence of different methodological approaches used to capture the jet position trends. A major limitation of most research into jet stream trends is a reliance on a single statistic to determine jet latitude position. Each statistic has assumptions about the appro-

64 primate region, vertical level and temporal resolution with which to capture the structure
 65 and/or climatology of a given jet stream within a given time window (Keel et al., 2024).

66 In this research, we examine climatological-scale trends of the lower tropospheric
 67 North Pacific Jet (NPJ) and assess the relative importance of the associated uncertain-
 68 ties in estimating its position. To do this, we define and assess four types of uncertainty:
 69 (a) *metric uncertainty* arising from uncertainty about the choice of jet statistic, (b) *model*
 70 *uncertainty* arising from the choice of model, (c) *internal variability* arising from spread
 71 amongst the realisation of the same climate model, and (d) *scenario uncertainty* aris-
 72 ing from uncertainty about forcing trajectories.

73 2 Data and Methods

74 2.1 Data

75 We use daily u -component wind speed data (in ms^{-1}) between 1st January 1980
 76 and 31st December 2021 from four modern climate reanalysis datasets: ERA5 (Hersbach
 77 et al., 2020), JRA-55 (Kobayashi et al., 2015), MERRA-2 (Global Modeling and Assimi-
 78 lation Office, 2015) and NCEP DOE II (Kanamitsu et al., 2002). A standardised North
 79 Pacific region (120–240°W, 20–70°N) is adopted at two pressure levels: 800 and 700 hPa.
 80 All data is processed at its native resolution.

81 Daily u -component wind (in ms^{-1}) were also retrieved from 28 models from 16 mod-
 82 elling groups of the Coupled Model Intercomparison Project Phase 6 (CMIP6; Eyring
 83 et al., 2016) for the *historical*, *SSP1-2.6*, *SSP2-4.5*, *SSP3-7.0*, *SSP5-8.5* experiments. Where
 84 available, multiple realisations of each simulation were obtained. A full list of models and
 85 realisations used in this study is provided in Table S1.

86 We also extract monthly mean temperature and all vertical levels of u -component
 87 wind for this period from ERA5 (Hersbach et al., 2020). From this monthly data, we cal-
 88 culate three climate indices introduced in Manzini et al. (2014) and modified by Oudar
 89 et al. (2020):

- 90 1. Arctic Amplification (AA): zonal mean temperature change between 1000–700 hPa
 91 and 60–90°N.
- 92 2. Tropical Amplification (TA): zonal mean temperature change between 400–150
 93 hPa and 20°S to 20°N.
- 94 3. Polar Vortex Strength (PVS): zonal mean u -component wind change between 250–30
 95 hPa and 70–90°N.

96 We express each of these indices as an anomaly relative to 1980–2022. Data for a fourth
 97 climate index, Monthly Pacific Decadal Oscillation (PDO; Mantua et al., 1997), were re-
 98 trieved for the period from the KNMI Climate Explorer (<https://climexp.knmi.nl>, Trouet
 99 & Van Oldenborgh, 2013).

100 2.2 Analysis techniques

101 We use seven different jet statistics to extract a jet latitude from zonal wind speed
 102 (Table 1). These statistics have been chosen based on their popularity and similarity of
 103 scope (to extract a single value of jet latitude in lower tropospheric winds), and each are
 104 available in Python’s *jsmetrics* package (Keel et al., 2024). These methods were primar-
 105 ily developed for low-level (500–925 hPa) zonal winds, making them more appropriate
 106 for assessing the eddy-driven components.

107 We compute each statistic on the standardised North Pacific region (regardless of
 108 the original metric definition). Each metric also estimates jet speed, but this analysis
 109 focuses only on jet position. Zappa et al. (2018), here Z18, initially developed for monthly

Table 1. Jet latitude statistics used in this study. The original methodology provides all pressure levels and temporal specifications. All statistics are included in the *jsmetrics* Python package (Keel et al., 2024).

Code	Study	hPa	Temporal	Method
W10	Woollings et al. (2010)	700-925	Daily	Lanczos low-pass filter then Fourier filter over max wind speed
BP13	Barnes and Polvani (2013)	700-850	Daily	Low-pass filter then quadratic interpolation
GP14	Grise and Polvani (2014)	850	Daily	Quadratic interpolation of max wind speed
BS17	Barnes and Simpson (2017)	700	10-day	Maximum wind speed
B18	Bracegirdle et al. (2018)	850	Annual	Cubic-spline interpolation of max wind speed
Z18	Zappa et al. (2018) ¹	850	Monthly	Centroid of wind speed profile
K20	Kerr et al. (2020) ²	500	Daily	Smoothed max wind speed by longitude

¹ Adapted from Ceppi et al. (2018); ² Adapted from Barnes and Fiore (2013)

110 resolution data, is calculated at a daily resolution in this research using *jsmetrics* (Keel
 111 et al., 2024). B18 was developed for seasonal and annual means, so it is not included in
 112 the comparison of monthly jet latitude.

113 We use a Mann-Kendall test to analyse jet position trends. This test looks for mono-
 114 tonically increasing or decreasing trends, and the null hypothesis is that no monotonic
 115 trend exists. We use a Mann-Whitney U test for differences to determine shifts in the
 116 jet position between two time periods. The null hypothesis is that no difference exists
 117 between the two samples. Finally, we use a Gaussian Kernel Density Estimation to gen-
 118 erate the probability density function of jet latitude trends and shifts.

119 3 Results

120 3.1 Observational trends in the North Pacific Jet position

121 Between 1980-2022, a weak negative correlation is shown between the record of each
 122 of the jet statistics and PDO ($\tau=-0.12$ to -0.18), as determined by Kendall's τ correla-
 123 tion coefficient (Figure 1). Although there are increasing trends in the Arctic and Trop-
 124 ical Amplification indices, they show a non-significant correlation with the jet statistics.

125 A linear poleward trend in the latitude of the low-level NPJ is shown in the record
 126 of each jet statistic, varying between 0.22-0.30°N per decade. However, this poleward
 127 trend is only a statistically significant monotonic increase using GP14, Z18, and K20.
 128 Estimates of the jet latitude vary between the methods, with the jet latitude from K20
 129 being relatively more poleward than the other statistics (see 43° N dashed line). Esti-
 130 mates from B18 indicate that the annual jet position has become increasingly narrow,
 131 and this has also been suggested in modelling research as forced by a tug of war on the
 132 jet stream between AA-TA (e.g. Peings et al., 2018, who look at the narrowing of the
 133 winter North Atlantic Jet).

134 Next, the NPJ position trend is separated into four seasons and with four climate
 135 reanalyses (Figure 2). By introducing additional reanalyses here, we can quantitatively

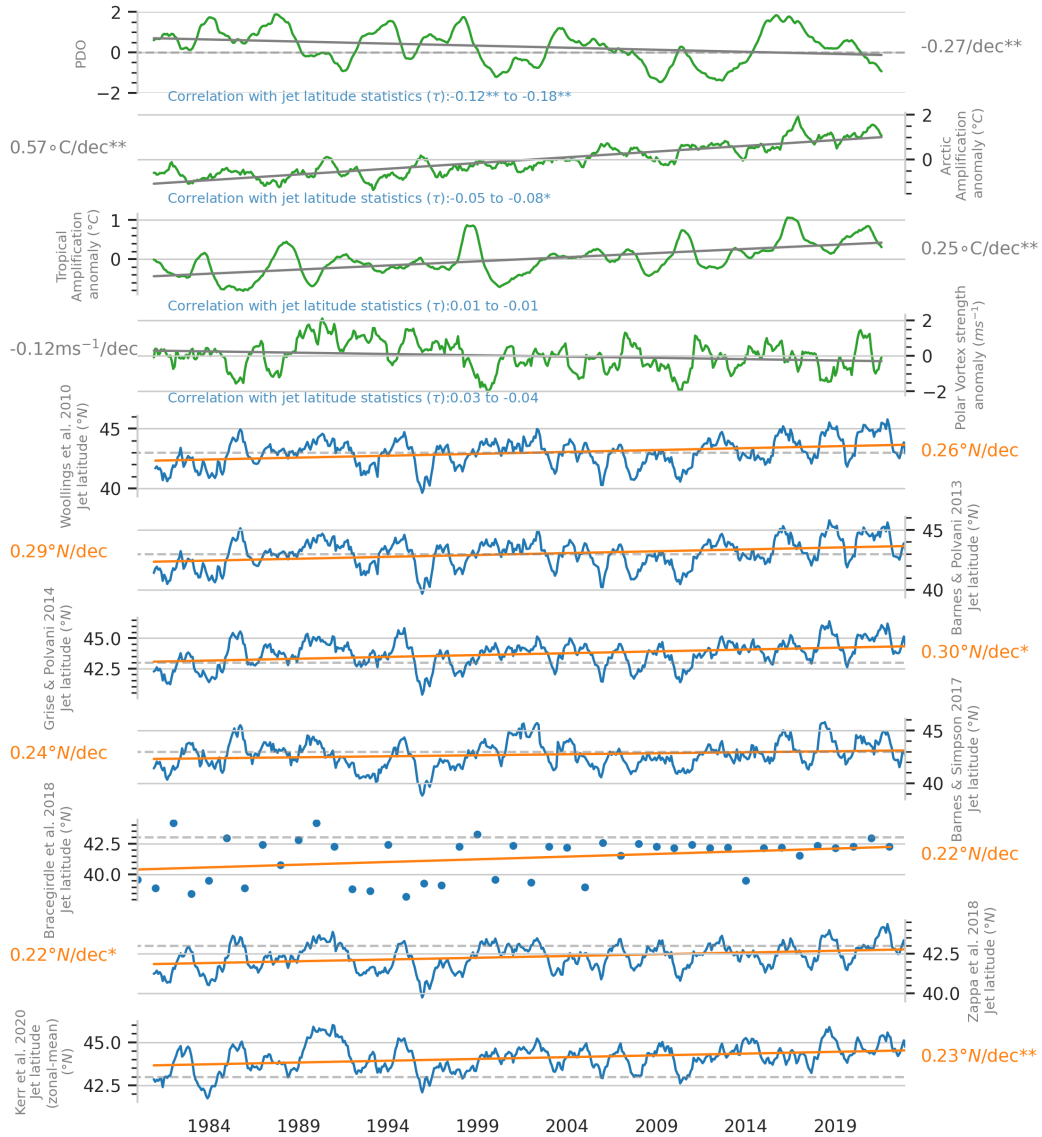


Figure 1. Annually smoothed monthly-mean trends of four climate indices and seven jet latitude statistics (B18 is one value per year) over a standardised North Pacific region calculated using ERA5 (Hersbach et al., 2020). A linear regression is drawn through each variable, and the slope is presented by year. Mann-Kendall tests are run for each variable, and their p-values are expressed next to the slope (* $p < 0.05$, ** $p < 0.01$). Kendall's Tau correlation coefficients are provided to show the range of correlation between each of the four climate indices and the jet statistics, except B18 (* $p < 0.05$, ** $p < 0.01$). For each jet statistic, a grey dashed line is drawn at 43°N.

136 compare the relative importance of *metric* and *model uncertainty* in estimating the jet
 137 latitude trend between 1980-2021. For every season except DJF, there is some uncertainty
 138 in the sign of the observational trend (i.e. at least one statistic-observation combination
 139 shows an equatorward trend) with JJA expressing the largest spread (-0.07–0.74 °N per
 140 decade; Figure 2c). Yet in DJF, when the climatological average jet is furthest south and
 141 is most closely linked to the edge of the Hadley Cell (e.g. Park & An, 2014), the trend
 142 of the NPJ latitude is shown to have been moving poleward between 0.34–0.85°N per
 143 decade (Figure 2a). The poleward DJF trend is statistically significant when examined
 144 using every combination of reanalysis and jet latitude statistics.

145 In each season, the jet latitude statistic used (i.e. the *metric uncertainty*) has a larger
 146 influence than which reanalysis is used (i.e. the *model uncertainty*) for the estimation
 147 of the jet latitude trend. We quantify reanalysis and model uncertainty by calculating
 148 the maximum and minimum trend in jet latitude with a fixed metric but different re-
 149 analysis. We calculate metric uncertainty by calculating the difference in estimated trends
 150 for a fixed reanalysis but a different metric. In DJF, the metric uncertainty ranges from
 151 0.25-0.4°N per decade across the reanalyses and the model uncertainty ranges from 0.12-
 152 0.20°N per decade across the metrics. In comparing these two ranges, we can determine
 153 that the uncertainty in the choice of statistic in DJF lies outside, and is more than, the
 154 range of uncertainty from choice of reanalysis in DJF (i.e. by at least 0.05°N per decade).

155 In all the other seasons, model uncertainty is a lower value. The metric uncertainty
 156 ranges between 0.16-0.24°N per decade (MAM), 0.31-0.54°N per decade (JJA), and 0.14-
 157 0.29°N per decade (SON) and the model uncertainty ranges between 0.12-0.23°N per decade
 158 (MAM), 0.26-0.53°N per decade (JJA), and 0.08-0.21°N per decade (SON). The widest
 159 range of both metric and model uncertainty about the NPJ trend is in JJA, and this is
 160 the only season where the maximum model uncertainty is higher than the maximum met-
 161 ric uncertainty (occurring across the JRA-55) (Figure 2c). No pattern suggests that some
 162 metrics or reanalyses perform systematically better across the seasons or that an ide-
 163 alised metric-dataset combination exists.

164 3.2 Projections of the shift of the North Pacific Jet position

165 The end-of-century (2070-2100) annual NPJ position is shown to move further pole-
 166 ward under increased GHG forcing trajectories in CMIP6 ScenarioMIP, and this shift
 167 is irrespective of the metric used (Figure 3). Simulated jet latitudes exhibit an equator-
 168 ward bias annually when compared to the spread of the four modern reanalysis sets in
 169 accordance with findings from previous studies (e.g. Bracegirdle et al., 2022, and refer-
 170 ences therein). This annual equatorward bias is more pronounced in W10, BP13 and GP14,
 171 where the 5-year running mean and inter-annual variability of the reanalyses lies out-
 172 side the range of jet latitude estimation in the historical experiments (see purple and grey
 173 boxes in Figure 3). The equatorward bias also has seasonal and metric dependence, pri-
 174 marily shown in DJF and SON (Figures S1-S4). Figure 3 shows synchronicity in the multi-
 175 decadal variability in the reanalysis between all metrics, except BS17, when viewed as
 176 a 5-year running mean, unlike the monthly values in Figure 1. A poleward shift that in-
 177 creases under higher GHG emission scenarios is seen each season except JJA (Figures
 178 S1-S4), with the shift in SON the most pronounced across the metrics.

179 To compare the relative importance of the *internal variability*, *metric* and *model*
 180 uncertainty, we examine the shift in the NPJ latitude projected between 30 years in the
 181 historical (1985-2014) and SSP5-8.5 (2070-2100) experiments in Figure 4. In this figure,
 182 the 28 models are ordered in descending order regarding future mean shift, and the colour
 183 denotes their similarity to the four reanalyses. We found no clear relationships between
 184 the similarity of any given model to the four reanalyses and the extent of the jet shift
 185 shown (Figure 4a). The majority of the models have an equatorward bias. While the ob-
 186 servational trend of the NPJ was found to be poleward in DJF (Figure 2a), across the

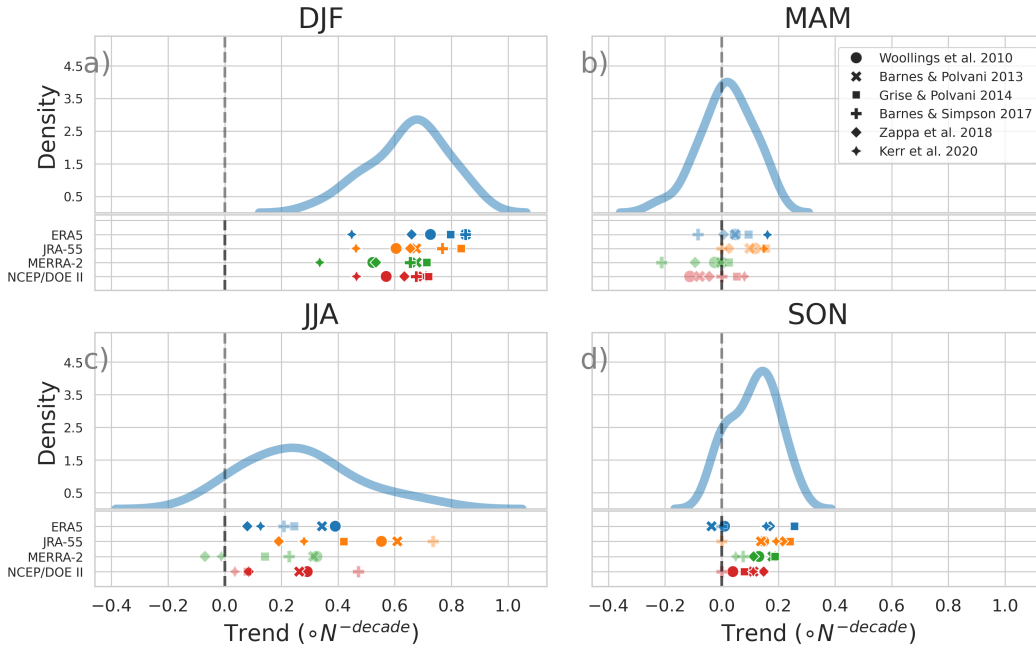


Figure 2. Kernel density estimates of the decadal trend of the North Pacific Jet latitude between 1st January 1980 and 31st December 2021 for each of four seasons, as estimated by four modern climate reanalysis products and six jet latitude statistics. Transparency indicates the statistical significance of the monotonic trend, as determined by a Mann-Kendall test. Opaque symbols indicate that the trend is statistically significant ($p < 0.05$).

187 models, there is no certainty about the sign of a shift in the annual mean (2.5%-97.5%
 188 confidence interval: -0.42 – 1.93°N) or within in any season at the end-of-century under
 189 the stronger GHG forcing scenario. The projected shift was found to be most poleward
 190 in SON, versus the other seasons, within the 2.5%-97.5% confidence interval (-0.25 – 2.63°N ;
 191 Figure 4a).

192 The end-of-century DJF jet latitude shift is compared by metric across the mod-
 193 els and by model across the statistics in the second and third panels of Fig 4a. The shift
 194 is generally associated with greater *model* uncertainty than *metric* uncertainty ([CHRIS
 195 CHECK] and the same is true for SON, see Figure S5). The projection of the shift varies
 196 between -0.76 – 2.6°N (95 PI; mean 0.89) across all the jet statistics and between -1.56 –
 197 3.47°N (mean 0.89) across the CMIP6 models (-0.85 – 2.9°N when using realisation mean).
 198 W10, BP13, GP14 and BS17 express a similar mean (within 0.04°N), and the major-
 199 ity of the models have a well-confined statistical range of 0.26 – 1.71°N (mean 0.74°N ;
 200 0.26 – 1.16°N if NorESM2-MM is excluded).

201 In Fig 4b&c, we examine models with multiple realisations to compare *initial con-*
 202 *dition uncertainty* in DJF and SON, the two seasons with the strongest poleward shifts.
 203 Generally, there is a relatively large amount of spread within realisations of an individ-
 204 ual model estimating future mean shift, varying between 0.79 – 2.9°N (mean 1.93°N) for
 205 DJF and 0.79 – 2.7°N (mean 1.7°N) for SON. There is some indication that different runs
 206 have a varying degree of associated metric uncertainty. For DJF, HadGEM3-GC31-MM
 207 is the only model where all the realisations of the model show a statistically significant
 208 difference ($p < 0.05$; determined by a Mann-Whitney U test for differences) across all statis-
 209 tics used. For SON, 6 out of the 10 multi-realisation models show a statistically signif-
 210 icant difference across all realisations and statistics used. We also ran the Mann-Whitney

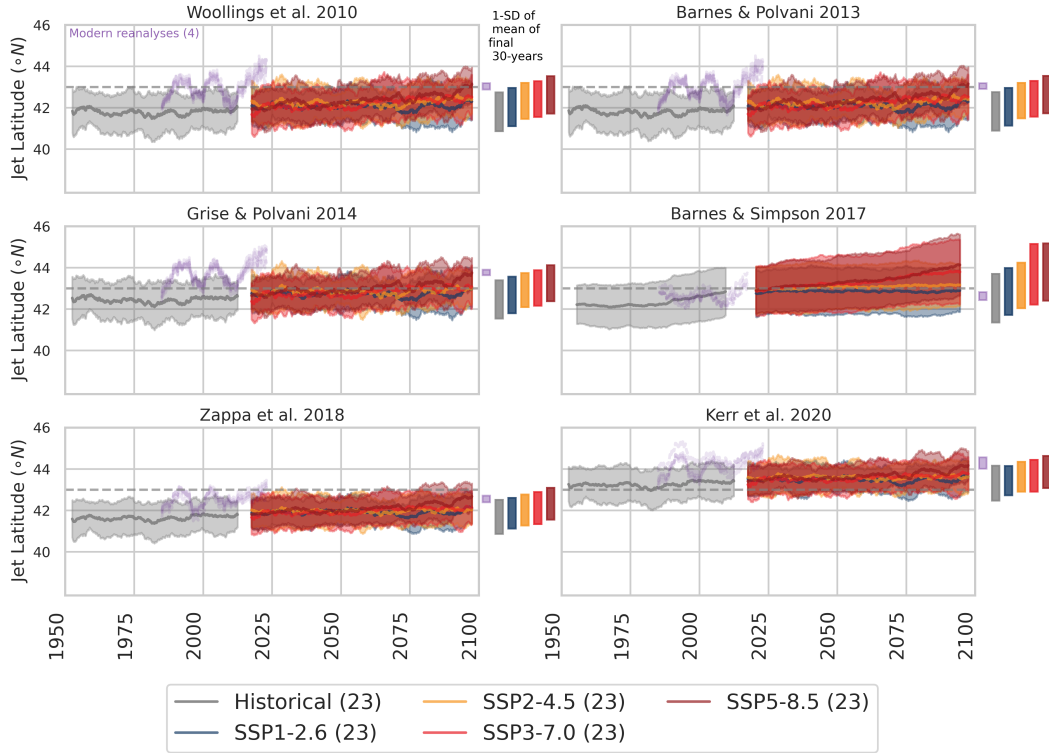


Figure 3. 5-year running mean projections of North Pacific Jet latitude with 5-year running standard deviation envelope. Each CMIP6 experiment contains outputs from the same 23 models. Purple lines represent the 5-rolling running mean from ERA5, JRA-55, MERRA 2 and NCEP DOE II reanalysis datasets between 1st January 1980 and 31st December 2021. Bars in each subplot relate to the standard deviation range about the mean of the last 30 years of the given model output. For each jet statistic, a grey dashed line is drawn at 43°N as in Fig. 1.

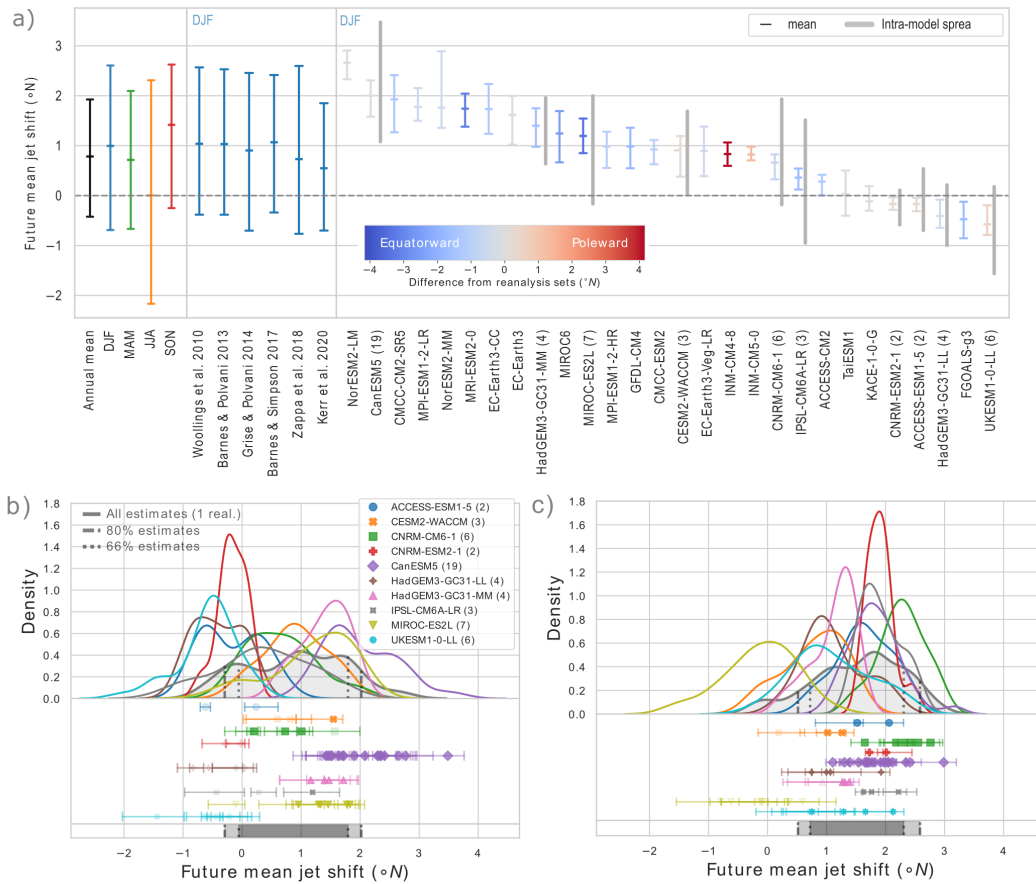


Figure 4. (a) Comparison of the end-of-century North Pacific Jet position shift between SSP5-8.5 (2070-2100) and Historical (1985-2014) experiments by annual mean and season (first panel), by metric (DJF only; second panel) and by CMIP6 model (DJF only; third panel). The height of each error bar represents the 2.5%-97.5% confidence interval, and the middle marker represents the mean. Grey bars represent the 2.5%-97.5% confidence interval of the ensemble spread of all estimations in models with multiple realisations. For these multi-realisation models, the error bar represents the spread of the means. Colour represents the difference between each model’s mean estimation and the reanalyses mean for each metric. Kernel density estimation of DJF (b) and SON (c) mean jet position shifts between the end-of-century SSP5-8.5 (2070-2100) and Historical (1985-2014) experiments within multi-realisation CMIP6 models. The error bar of each realisation within the modelling groups represents the range of estimates produced by the six jet statistics, with the markers representing the mean of those values. Transparency of the marker is used to signify the statistical significance of a Mann-Whitney U test. Opaque symbols signify that the trend is statistically significant ($p < 0.05$). Grey bars represent the area between the 10th and 90th percentile (80% of the models) and 17th and 83rd percentile (66% of the models) of one run from each of the 28 CMIP6 models used in this analysis.

U test for differences across all the realisations of all models and found between 50-68 (depending on the statistic used) out of 75 models show a statistically significant difference in DJF, and between 64-70 models show a statistically significant difference in SON.

Using one realisation from each of the 28 CMIP6 models available, we find the future mean jet shift projected to be within -0.29 - 1.80°N in DJF and within 0.52 - 2.58°N in SON within 80% of the models. As such, there is a significant agreement about the poleward shift in SON of the NPJ and a general leaning towards poleward shift for DJF (Fig 4b&c).

4 Discussion and Conclusions

In this study, we found that the observed wintertime North Pacific Jet (NPJ) has been moving polewards at a rate of 0.34 - 0.85°N per decade between 1980-2022, and this trend is robust to any combination of jet statistics and reanalysis. Consistent with recent research in other regions (e.g. Martin, 2021; Woollings et al., 2023), it is likely that the gradual extension of the data record, up to 2022 here, is producing significant trends which are emerging outside of natural variability in winter. Consistent with recent research in other regions (e.g. Martin, 2021; Woollings et al., 2023), it is likely that the gradual extension of the data record, up to 2022 here, is producing significant trends which are emerging outside of natural variability in winter. These trends also appear clearest in the most recent decades, so the trend may not exist with the last decade removed from the record (e.g. see discussion of similar work done on trends in jet waviness in Blackport & Screen, 2020).

No direct correlation was found between the NPJ position and tropical or Arctic amplification or polar vortex strength in this time frame, so we do not discover any immediate causation for these trends. While this seemingly opposes what we may expect in modelling research, it is likely that these dynamics of these forcing on the position of the NPJ have not yet become fully apparent in the observational record, or have only recently emerged from natural variability (Peings et al., 2018; Woollings et al., 2023). The influence of the tug-of-war between AA-TA and the changes to the Polar Stratosphere have all been shown to control the climatological jet position in modelling studies (Peings et al., 2019). However, to study the dynamical relationship between broader climate change and the shifting or narrowing (e.g. Peings et al., 2018) of the NPJ would require a more detailed study of causation (Oudar et al., 2020). Additionally, recent work has proposed a mechanism that relates this poleward trend in the wintertime NPJ to the observed movement of the northern edge of the Hadley Cell (Menzel et al., 2024).

Using CMIP6 ScenarioMIP, we found the annual position of the NPJ to continue to extend poleward, consistent with findings of the movement of lower tropospheric jet streams and upper level zonal winds (e.g. Rivière, 2011; Harvey et al., 2020; Oudar et al., 2020). We found an equatorward bias of the CMIP6 versus the reanalyses, also shown in previous studies (e.g. Harvey et al., 2020; Oudar et al., 2020). We see no clear pattern between the shift shown in the models and the similarity to the four reanalysis sets. The extent to which this bias in CMIP6 obfuscates the NPJ latitude shift requires further research, but we were able to indicate that there is also a metric uncertainty associated with the extent of this bias in the North Pacific (Figure 3).

A robust poleward shift is seen in the SON end-of-century North Pacific jet position in SSP5-8.5 that is robust to *internal variability* and *metric, model* uncertainty. However, there is still some uncertainty about the magnitude of the shift varying between 0.5 - 2.6°N considering the 2.5%-97.5% confidence interval of the models. The inter-model spread has a larger relative uncertainty than the metric choice in estimating this shift. Moreover, as with most analyses, we demonstrate that statistics are still important when studying the North Pacific jet.

In conclusion, we have indicated that using multiple statistics developed for a similar purpose in a standardised manner can be useful for assessing the uncertainty in estimating the climatological jet. The NPJ is coupled to surface conditions through heat and moisture transport and the storm tracks (Shaw et al., 2016), so understanding how its mean position is changing (regardless of whether direct causation to larger climatic changes can be drawn) is vital for understanding the trajectory of the mid-latitude climate in the 21st century.

5 Availability Statement

The data that support the findings of this study are openly available at the following URL/DOIs: CMIP6 from <https://esgf-index1.ceda.ac.uk/projects/esgf-ceda/>; ERA5 hourly from <https://doi.org/10.24381/cds.bd0915c6>; JRA-55 daily from <https://doi.org/10.5065/D6HH6H41>; MERRA-2 daily from https://gmao.gsfc.nasa.gov/reanalysis/MERRA-2/data_access/; NCEP-DOE II daily from <https://ps1.noaa.gov/data/gridded/data.ncep.reanalysis2.html>.

The jsmetrics software is available from <https://zenodo.org/doi/10.5281/zenodo.7081633> and documentation for the software is provided at <https://jsmetrics.readthedocs.io/en/latest/index.html>.

The IPython notebooks to reproduce the figures of this manuscript are available at <https://zenodo.org/doi/10.5281/zenodo.10877210>. And the analysis runner to run jsmetrics in batch on JASMIN is available at <https://zenodo.org/doi/10.5281/zenodo.10876824>.

Acknowledgments

This work was funded by the Natural Environment Research Council (grant no. NE/S007229/1). TK is grateful for NERC funding through the London NERC Research Doctoral Training Partnership.

We thank the climate modelling groups for producing and making available their model output, the Earth System Grid Federation (ESGF) for archiving the data and providing access, and the multiple funding agencies that support CMIP6 and ESGF. This work used JASMIN, the UK collaborative data analysis facility.

We would also like to thank Alan Iwi at the CEDA Helpdesk for arranging a data transfer to JASMIN, which extended this analysis.

References

- Archer, C. L., & Caldeira, K. (2008, 4). Historical trends in the jet streams. *Geophysical Research Letters*, *35*(8), L08803. Retrieved from <http://doi.wiley.com/10.1029/2008GL033614> doi: 10.1029/2008GL033614
- Barnes, E. A., & Fiore, A. M. (2013). Surface ozone variability and the jet position: Implications for projecting future air quality. *Geophysical Research Letters*, *40*(11), 2839–2844. doi: 10.1002/grl.50411
- Barnes, E. A., & Polvani, L. (2013, 9). Response of the midlatitude jets, and of their variability, to increased greenhouse gases in the CMIP5 models. *Journal of Climate*, *26*(18), 7117–7135. Retrieved from <http://journals.ametsoc.org/doi/10.1175/JCLI-D-12-00536.1> doi: 10.1175/JCLI-D-12-00536.1
- Barnes, E. A., & Simpson, I. R. (2017, 12). Seasonal Sensitivity of the Northern Hemisphere Jet Streams to Arctic Temperatures on Subseasonal Time Scales. *Journal of Climate*, *30*(24), 10117–10137. Retrieved from <https://journals.ametsoc.org/doi/10.1175/JCLI-D-17-0299.1> doi:

- 10.1175/JCLI-D-17-0299.1
- Blackport, R., & Screen, J. A. (2020, 2). Insignificant effect of Arctic amplification on the amplitude of midlatitude atmospheric waves. *Science Advances*, *6*(8), eaay2880. Retrieved from <https://advances.sciencemag.org/lookup/doi/10.1126/sciadv.aay2880> doi: 10.1126/sciadv.aay2880
- Bracegirdle, T. J., Hyder, P., & Holmes, C. R. (2018). CMIP5 diversity in Southern Westerly jet projections related to historical sea ice area: Strong link to strengthening and weak link to shift. *Journal of Climate*, *31*(1), 195–211. doi: 10.1175/JCLI-D-17-0320.1
- Bracegirdle, T. J., Lu, H., & Robson, J. (2022, 1). Early-winter North Atlantic low-level jet latitude biases in climate models: implications for simulated regional atmosphere-ocean linkages. *Environmental Research Letters*, *17*(1), 014025. Retrieved from <https://iopscience.iop.org/article/10.1088/1748-9326/ac417f> doi: 10.1088/1748-9326/ac417f
- Ceppi, P., Zappa, G., Shepherd, T. G., & Gregory, J. M. (2018). Fast and slow components of the extratropical atmospheric circulation response to CO₂ forcing. *Journal of Climate*, *31*(3), 1091–1105. doi: 10.1175/JCLI-D-17-0323.1
- Cohen, J., Zhang, X., Francis, J., Jung, T., Kwok, R., Overland, J., ... Yoon, J. (2020). Divergent consensus on Arctic amplification influence on midlatitude severe winter weather. *Nature Climate Change*, *10*(1), 20–29. doi: 10.1038/s41558-019-0662-y
- Curtis, P. E., Ceppi, P., & Zappa, G. (2020). Role of the mean state for the Southern Hemispheric jet stream response to CO₂ forcing in CMIP6 models. *Environmental Research Letters*, *15*(6). doi: 10.1088/1748-9326/ab8331
- Eyring, V., Bony, S., Meehl, G. A., Senior, C. A., Stevens, B., Stouffer, R. J., & Taylor, K. E. (2016, 5). Overview of the Coupled Model Intercomparison Project Phase 6 (CMIP6) experimental design and organization. *Geoscientific Model Development*, *9*(5), 1937–1958. Retrieved from <https://gmd.copernicus.org/articles/9/1937/2016/> doi: 10.5194/gmd-9-1937-2016
- Global Modeling and Assimilation Office. (2015). *MERRA-2 instM_3d_asm_Np_3d, Monthly mean, Instantaneous, Pressure-Level, Assimilation, Assimilated Meteorological Fields V5.12.4*. Greenbelt, MD: Goddard Earth Sciences Data and Information Service Centre (GES DISC). doi: 10.5067/2E096JV59PK7
- Grise, K. M., & Polvani, L. M. (2014, 1). Is climate sensitivity related to dynamical sensitivity? A Southern Hemisphere perspective. *Geophysical Research Letters*, *41*(2), 534–540. Retrieved from <https://agupubs.onlinelibrary.wiley.com/doi/10.1002/2013GL058466> doi: 10.1002/2013GL058466
- Harvey, B. J., Cook, P., Shaffrey, L. C., & Schiemann, R. (2020). The Response of the Northern Hemisphere Storm Tracks and Jet Streams to Climate Change in the CMIP3, CMIP5, and CMIP6 Climate Models. *Journal of Geophysical Research: Atmospheres*, *125*(23), 1–10. doi: 10.1029/2020JD032701
- Hersbach, H., Bell, B., Berrisford, P., Hirahara, S., Horányi, A., Muñoz-Sabater, J., ... Thépaut, J. (2020, 7). The ERA5 global reanalysis. *Quarterly Journal of the Royal Meteorological Society*, *146*(730), 1999–2049. Retrieved from <https://onlinelibrary.wiley.com/doi/10.1002/qj.3803> doi: 10.1002/qj.3803
- Kanamitsu, B. Y. M., Ebisuzaki, W., Jack, W. O. O. L. L. E. N., Yang, S.-k., Hnilo, J. J., Fiorino, M., & Potter, G. L. (2002). NCEP-DOE AMIP-II Reanalysis (R-2). *Bulletin of the American Meteorological Society* (November), 1631–1643. doi: 10.1175/BAMS-83-11
- Keel, T., Brierley, C., & Edwards, T. (2024). jsmetrics v0.2.0 : a Python package for metrics and algorithms used to identify or characterise atmospheric jet streams. *Geoscientific Model Development*, *17*(3), 1229–1247. doi: <https://doi.org/10.5194/gmd-17-1229-2024>

- 362 Kerr, G. H., Waugh, D. W., Steenrod, S. D., Strode, S. A., & Strahan, S. E. (2020,
363 11). Surface Ozone-Meteorology Relationships: Spatial Variations and the Role
364 of the Jet Stream. *Journal of Geophysical Research: Atmospheres*, *125*(21), 1–
365 18. doi: 10.1029/2020JD032735
- 366 Kobayashi, S., Ota, Y., Harada, Y., Ebata, A., Moriya, M., Onoda, H., ... Taka-
367 hashi, K. (2015). The JRA-55 Reanalysis: General Specifications and Basic
368 Characteristics. *Journal of the Meteorological Society of Japan. Ser. II*, *93*(1),
369 5–48. Retrieved from [https://www.jstage.jst.go.jp/article/jmsj/93/1/
370 93_2015-001/article](https://www.jstage.jst.go.jp/article/jmsj/93/1/93_2015-001/article) doi: 10.2151/jmsj.2015-001
- 371 Lorenz, D. J., & DeWeaver, E. T. (2007). Tropopause height and zonal wind re-
372 sponse to global warming in the IPCC scenario integrations. *Journal of Geo-
373 physical Research Atmospheres*, *112*(10), 1–11. doi: 10.1029/2006JD008087
- 374 Lu, J., Vecchi, G. A., & Reichler, T. (2007). Expansion of the Hadley cell under
375 global warming. *Geophysical Research Letters*, *34*(February), 2–6. doi: 10
376 .1029/2006GL028443
- 377 Mantua, N. J., Hare, S. R., Zhang, Y., Wallace, J. M., & Francis, R. C. (1997).
378 A Pacific Interdecadal Climate Oscillation with Impacts on Salmon Produc-
379 tion. *Bulletin of the American Meteorological Society*, *78*(6), 1069–1079. doi:
380 10.1175/1520-0477(1997)078<1069:APICOW>2.0.CO;2
- 381 Manzini, E., Karpechko, A. Y., Anstey, J., Baldwin, M. P., Black, R. X., Cagnazzo,
382 C., ... Zappa, G. (2014, 7). Northern winter climate change: Assessment
383 of uncertainty in CMIP5 projections related to stratosphere-troposphere
384 coupling. *Journal of Geophysical Research: Atmospheres*, *119*(13), 7979–
385 7998. Retrieved from <http://doi.wiley.com/10.1002/2013JD021403> doi:
386 10.1002/2013JD021403
- 387 Martin, J. E. (2021, 5). Recent Trends in the Waviness of the Northern Hemisphere
388 Wintertime Polar and Subtropical Jets. *Journal of Geophysical Research:
389 Atmospheres*, *126*(9), 1–15. Retrieved from [https://onlinelibrary.wiley
390 .com/doi/10.1029/2020JD033668](https://onlinelibrary.wiley.com/doi/10.1029/2020JD033668) doi: 10.1029/2020JD033668
- 391 Menzel, M. E., Waugh, D. W., Wu, Z., & Reichler, T. (2024, 2). Replicating
392 the Hadley cell edge and subtropical jet latitude disconnect in idealized at-
393 mospheric models. *Weather and Climate Dynamics*, *5*(1), 251–261. Re-
394 trieved from <https://wcd.copernicus.org/articles/5/251/2024/> doi:
395 10.5194/wcd-5-251-2024
- 396 Oudar, T., Cattiaux, J., & Douville, H. (2020). Drivers of the Northern Extratrop-
397 ical Eddy-Driven Jet Change in CMIP5 and CMIP6 Models. *Geophysical Re-
398 search Letters*, *47*(8), 1–9. doi: 10.1029/2019GL086695
- 399 Park, J. H., & An, S. I. (2014). The impact of tropical western Pacific convection
400 on the North Pacific atmospheric circulation during the boreal winter. *Climate
401 Dynamics*, *43*(7-8), 2227–2238. doi: 10.1007/s00382-013-2047-7
- 402 Peings, Y., Cattiaux, J., & Magnusdottir, G. (2019). The Polar Stratosphere as
403 an Arbiter of the Projected Tropical Versus Polar Tug of War. *Geophysical Re-
404 search Letters*, *46*(15), 9261–9270. doi: 10.1029/2019GL082463
- 405 Peings, Y., Cattiaux, J., Vavrus, S. J., & Magnusdottir, G. (2018, 7). Projected
406 squeezing of the wintertime North-Atlantic jet. *Environmental Research Let-
407 ters*, *13*(7), 074016. Retrieved from [https://doi.org/10.1088/1748-9326/
408 aacc79](https://doi.org/10.1088/1748-9326/aacc79)<https://iopscience.iop.org/article/10.1088/1748-9326/aacc79>
409 doi: 10.1088/1748-9326/aacc79
- 410 Rivière, G. (2011). A dynamical interpretation of the poleward shift of the jet
411 streams in global warming scenarios. *Journal of the Atmospheric Sciences*,
412 *68*(6), 1253–1272. doi: 10.1175/2011JAS3641.1
- 413 Santer, B. D., Solomon, S., Pallotta, G., Mears, C., Po-Chedley, S., Fu, Q., ... Bon-
414 fils, C. (2017). Comparing tropospheric warming in climate models and satel-
415 lite data. *Journal of Climate*, *30*(1), 373–392. doi: 10.1175/JCLI-D-16-0333.1
- 416 Screen, J. A., Eade, R., Smith, D. M., Thomson, S., & Yu, H. (2022). Net Equa-

- 417 torward Shift of the Jet Streams When the Contribution From Sea-Ice Loss
418 Is Constrained by Observed Eddy Feedback. *Geophysical Research Letters*,
419 49(23), 1–9. doi: 10.1029/2022GL100523
- 420 Shaw, T. A., Baldwin, M., Barnes, E. A., Caballero, R., Garfinkel, C. I., Hwang,
421 Y.-T., . . . Voigt, A. (2016, 9). Storm track processes and the opposing influ-
422 ences of climate change. *Nature Geoscience*, 9(9), 656–664. Retrieved from
423 <http://www.nature.com/articles/ngeo2783> doi: 10.1038/ngeo2783
- 424 Stendel, M., Francis, J., White, R., Williams, P. D., & Woollings, T. (2021). The
425 jet stream and climate change. In Trevor M. Letcher (Ed.), *imate change* (3rd
426 ed., pp. 327–357). Elsevier. Retrieved from [https://linkinghub.elsevier](https://linkinghub.elsevier.com/retrieve/pii/B9780128215753000153)
427 [.com/retrieve/pii/B9780128215753000153](https://linkinghub.elsevier.com/retrieve/pii/B9780128215753000153) doi: 10.1016/B978-0-12-821575
428 -3.00015-3
- 429 Trouet, V., & Van Oldenborgh, G. J. (2013). KNMI climate explorer: A web-based
430 research tool for high-resolution paleoclimatology. *Tree-Ring Research*, 69(1),
431 3–13. doi: 10.3959/1536-1098-69.1.3
- 432 Vallis, G. K. (2019). *Essentials of Atmospheric and Oceanic Dynamics* (1st ed.).
433 Cambridge: Cambridge University Press.
- 434 Woollings, T., Drouard, M., O’Reilly, C. H., Sexton, D. M., & McSweeney, C.
435 (2023). Trends in the atmospheric jet streams are emerging in observations
436 and could be linked to tropical warming. *Communications Earth and Environ-*
437 *ment*, 4(1). doi: 10.1038/s43247-023-00792-8
- 438 Woollings, T., Hannachi, A., & Hoskins, B. (2010). Variability of the North Atlantic
439 eddy-driven jet stream. *Quarterly Journal of the Royal Meteorological Society*,
440 136(649), 856–868. doi: 10.1002/qj.625
- 441 Zappa, G., Pithan, F., & Shepherd, T. G. (2018). Multimodel Evidence for an
442 Atmospheric Circulation Response to Arctic Sea Ice Loss in the CMIP5
443 Future Projections. *Geophysical Research Letters*, 45(2), 1011–1019. doi:
444 10.1002/2017GL076096

Figure 3.

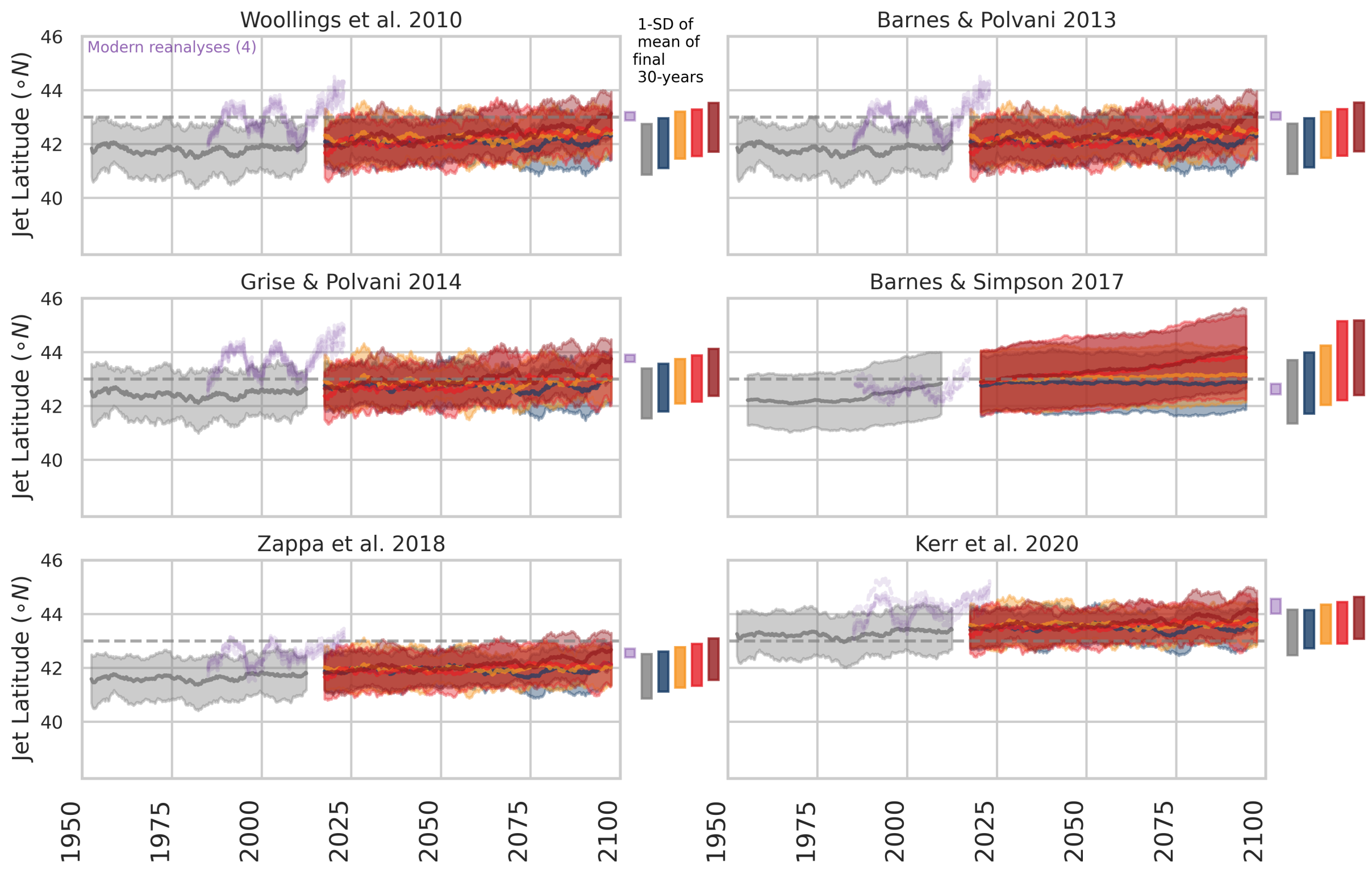
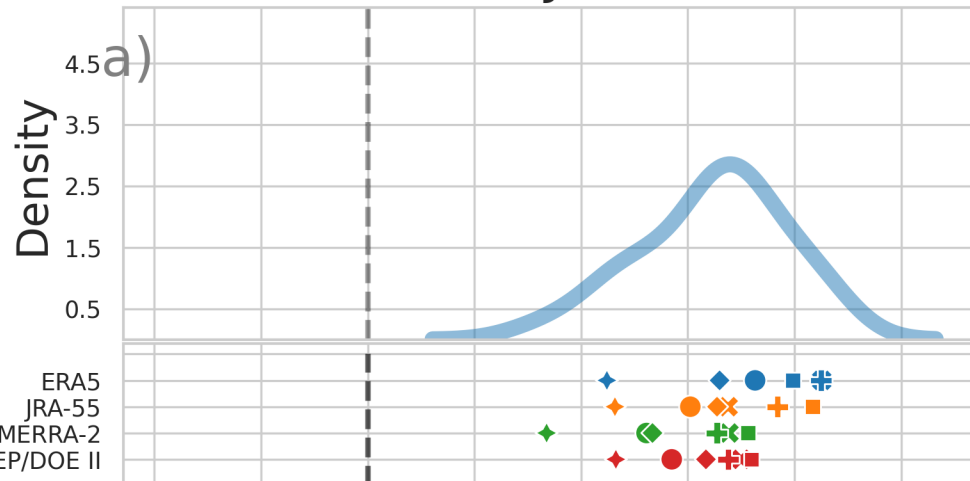
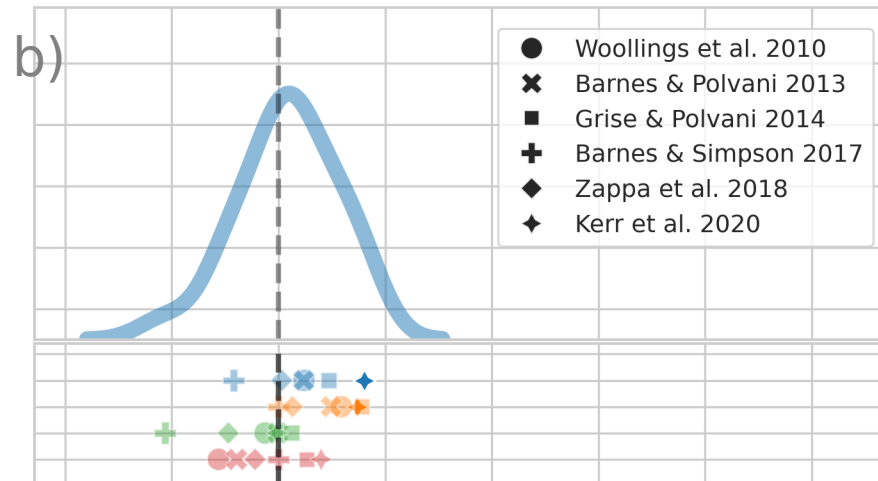


Figure 2.

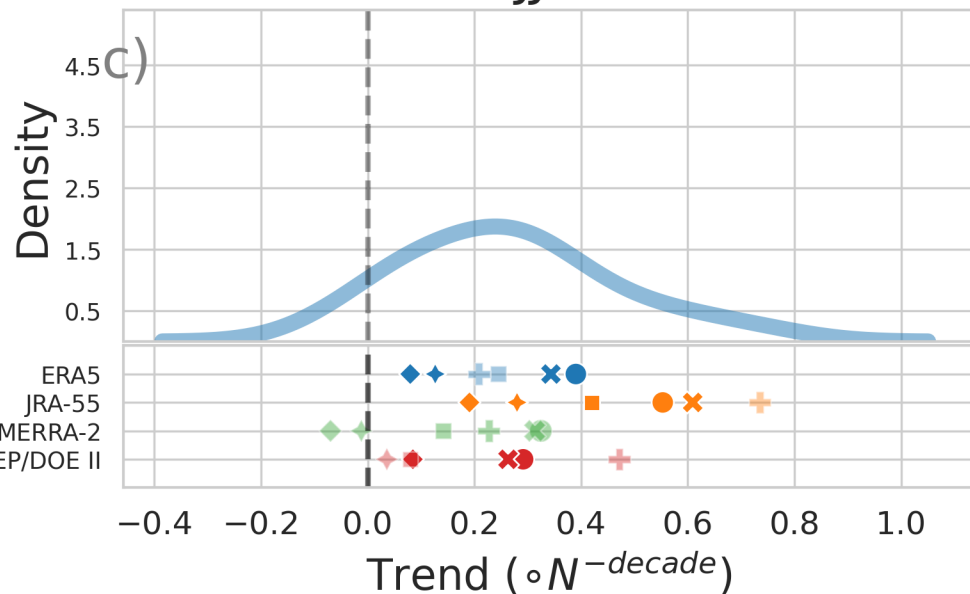
DJF



MAM



JJA



SON

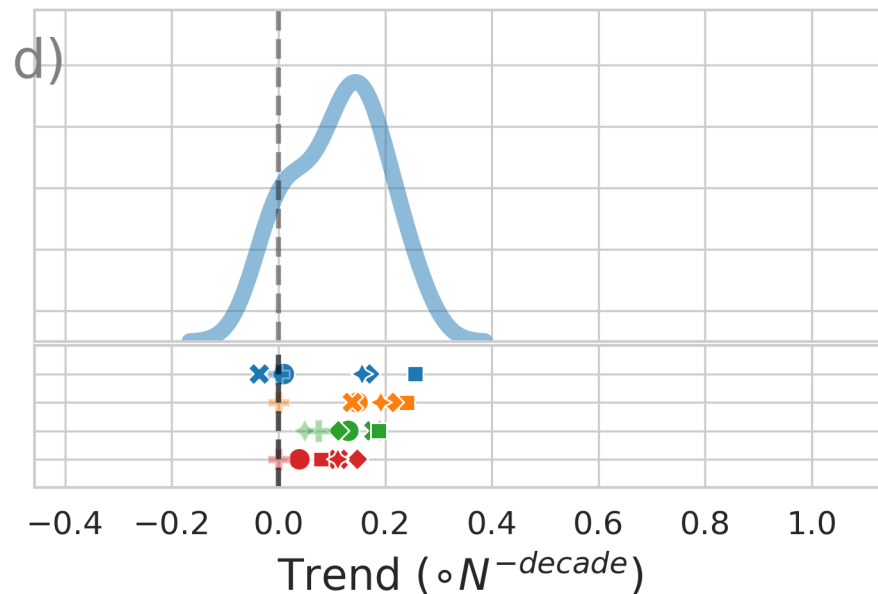


Figure 1.

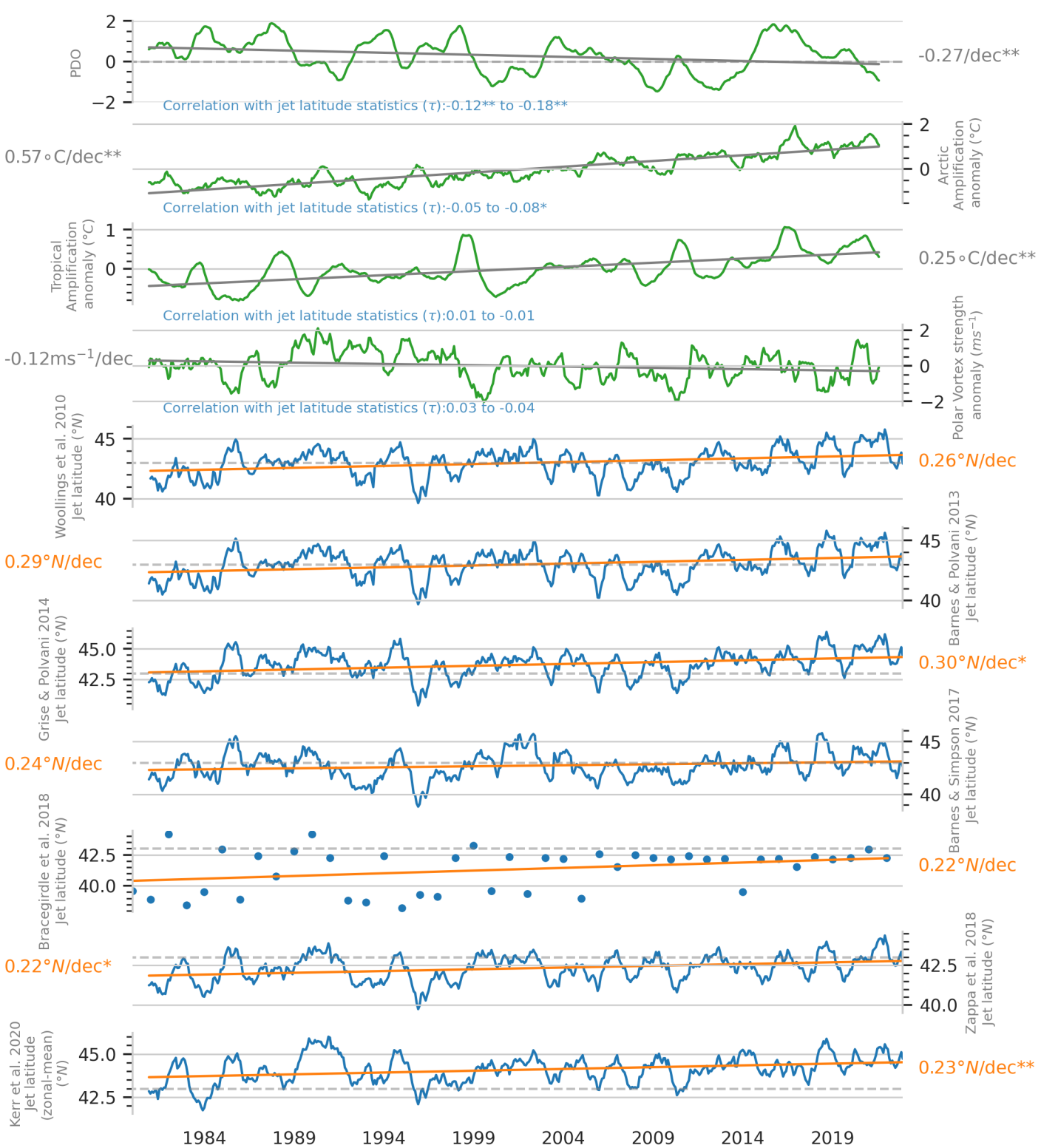
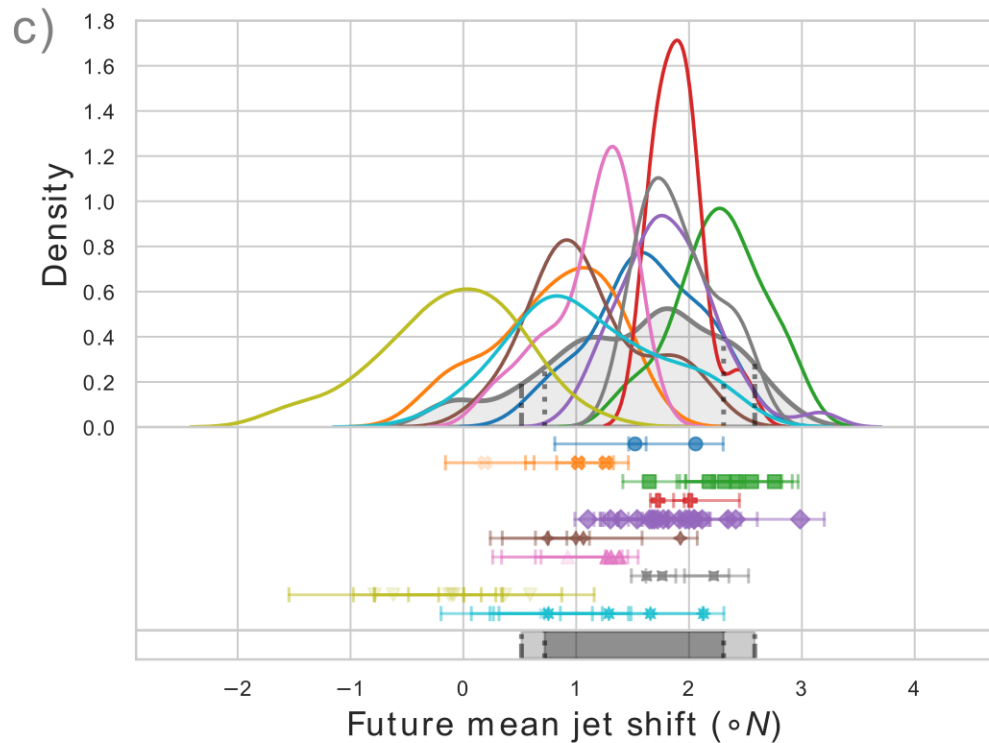
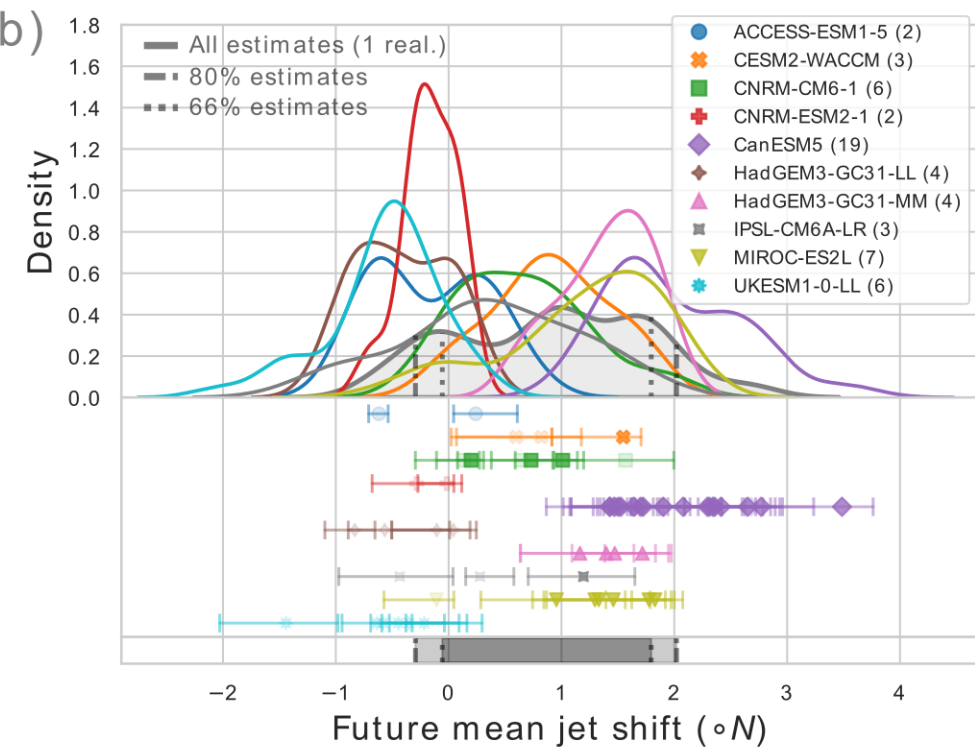
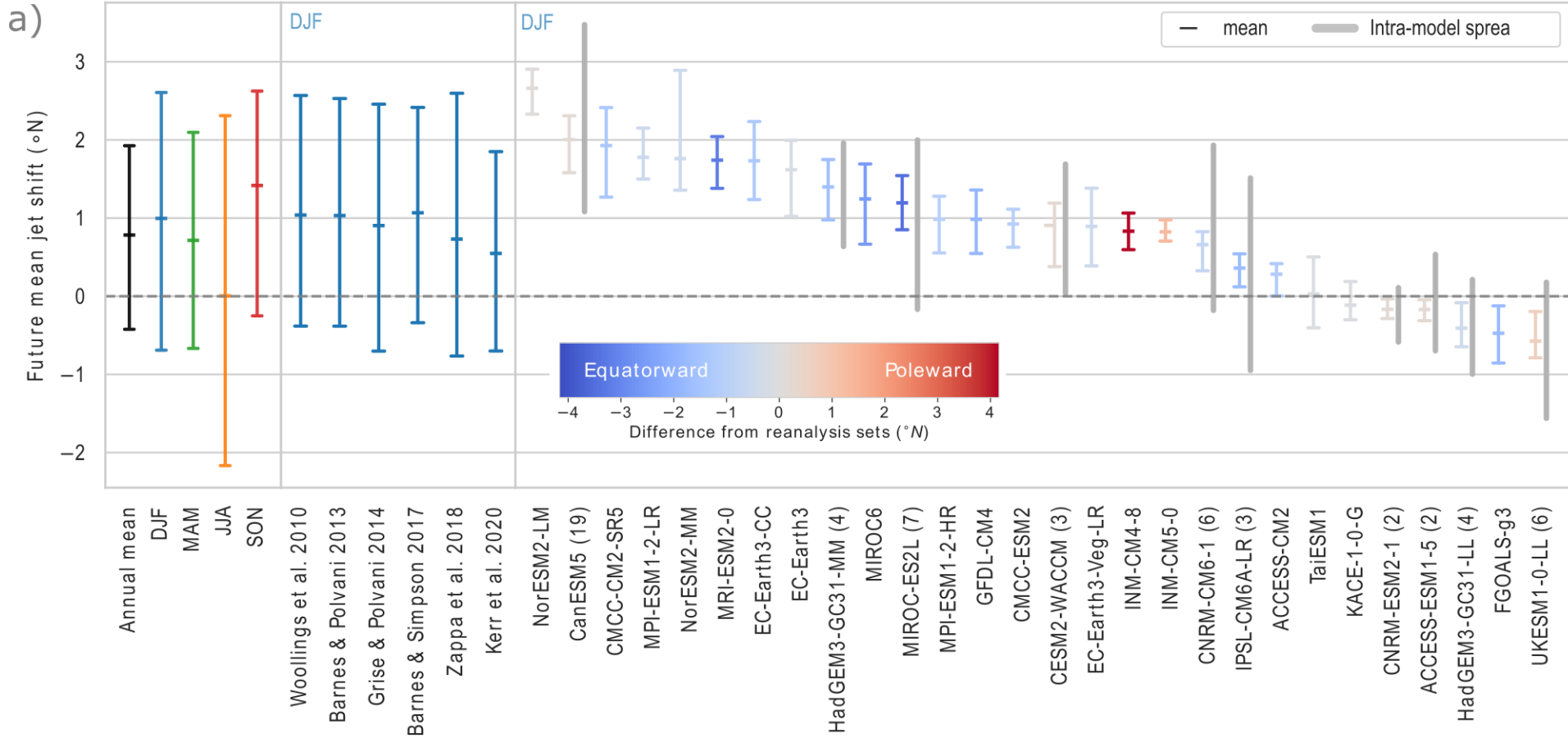


Figure 4.



Supporting Information for “Exploring uncertainty of trends in the lower-tropospheric North Pacific Jet position.”

Tom Keel^{1,2}, Chris Brierley¹, Tamsin Edwards² and Thomas H. A. Frame³

¹Department of Geography, University College London, Gower Street, London, WC1E 6BT

²Department of Geography, King's College London, 40 Bush House, London, WC2B 4BG

³Department of Meteorology, University of Reading, Reading, RG6 6ET

Contents of this file

1. Figures S1 to S5
2. Table S1

Figures S1 to S5

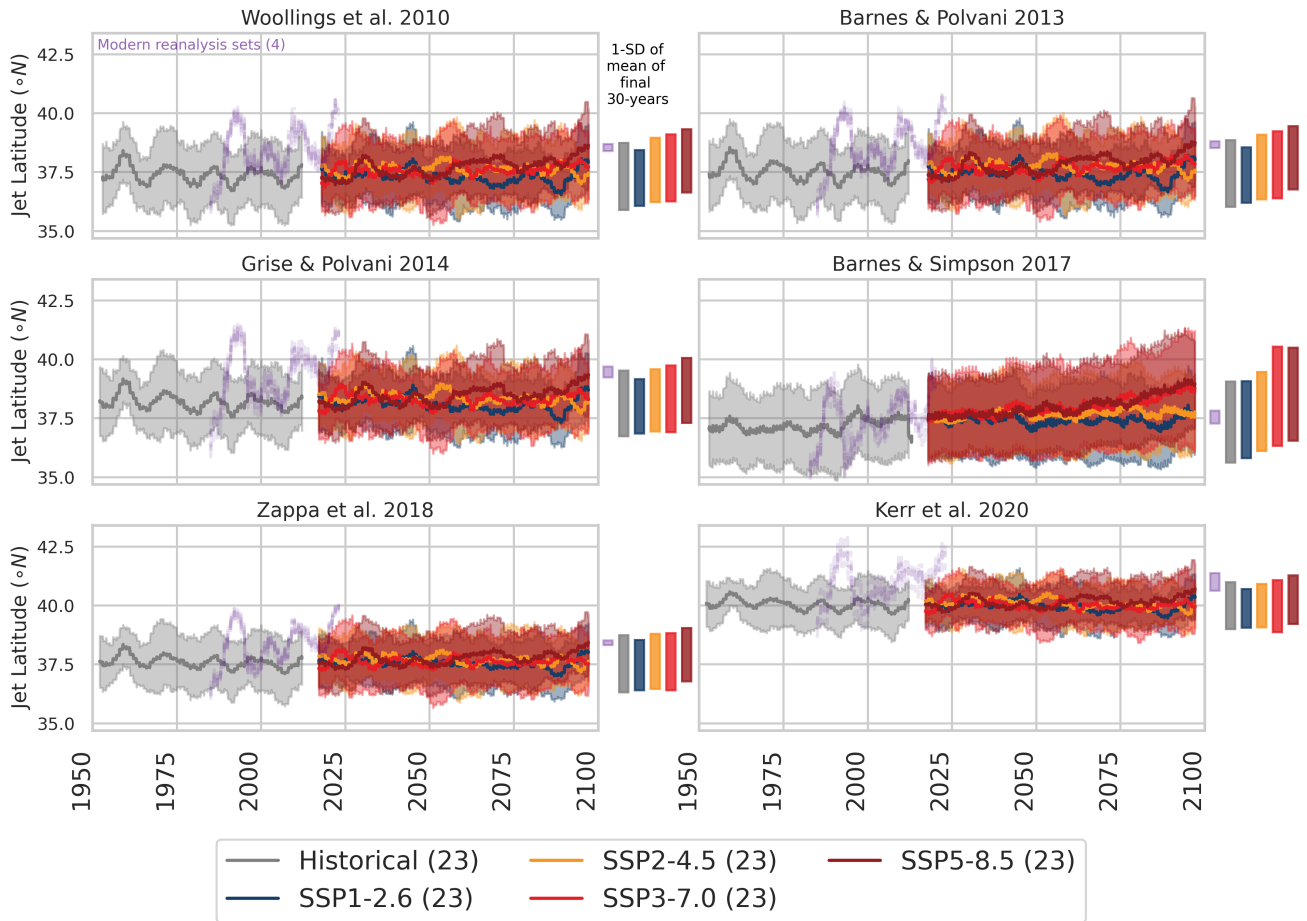


Figure S1. As for Fig. 3, but for Winter (DJF).

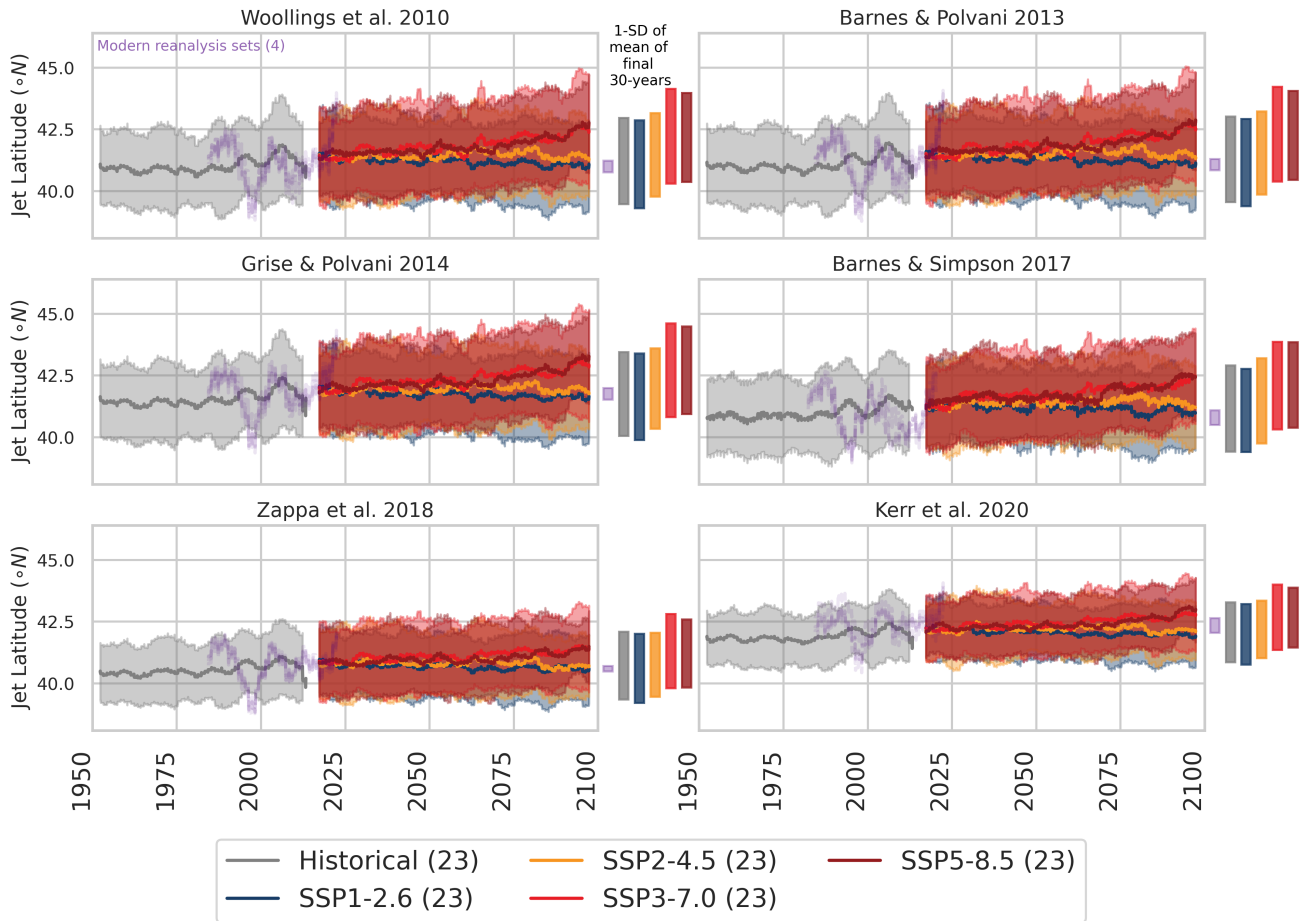


Figure S2. As for Fig. 3, but for Spring (MAM).

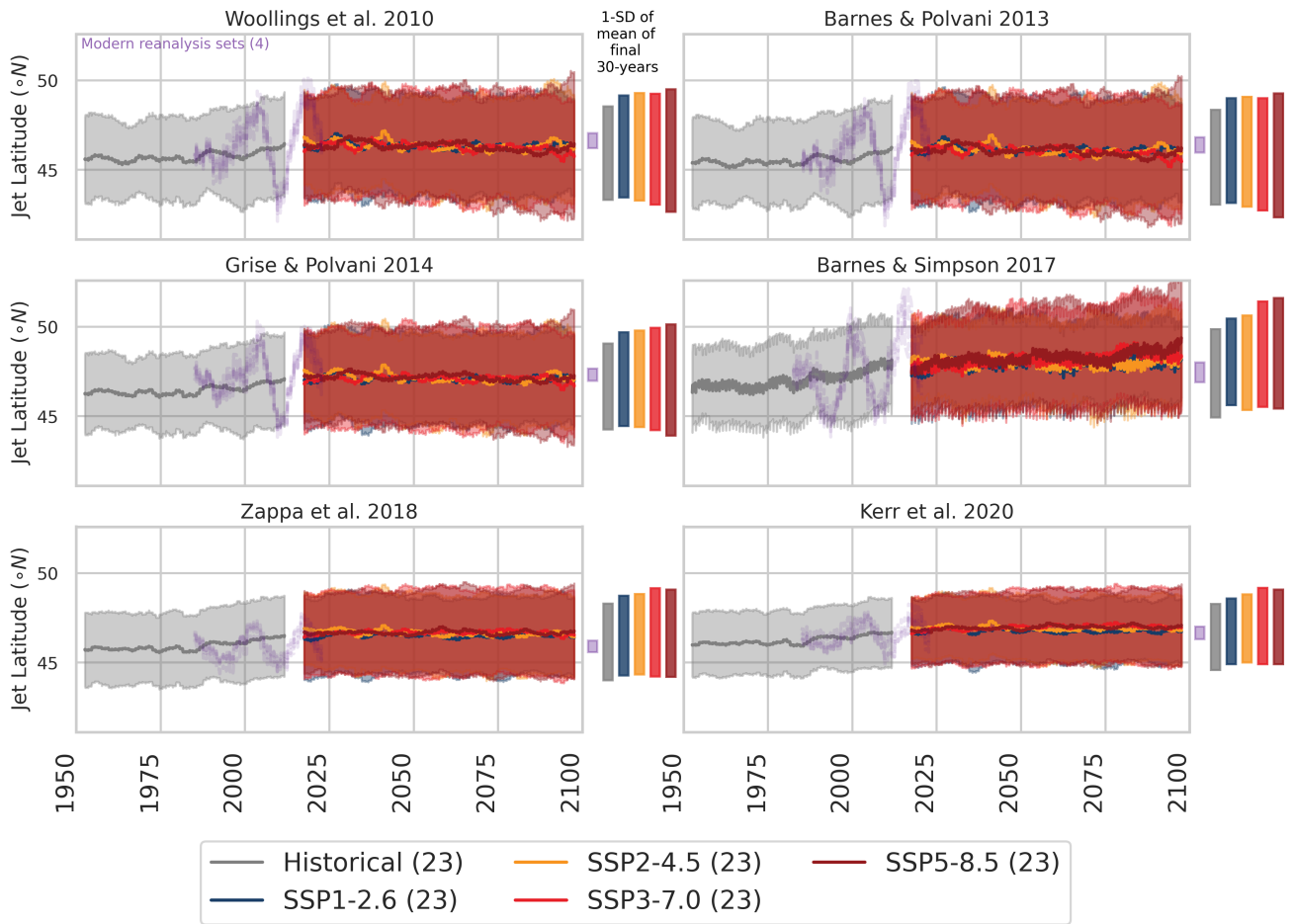


Figure S3. As for Fig. 3, but for Summer (JJA).

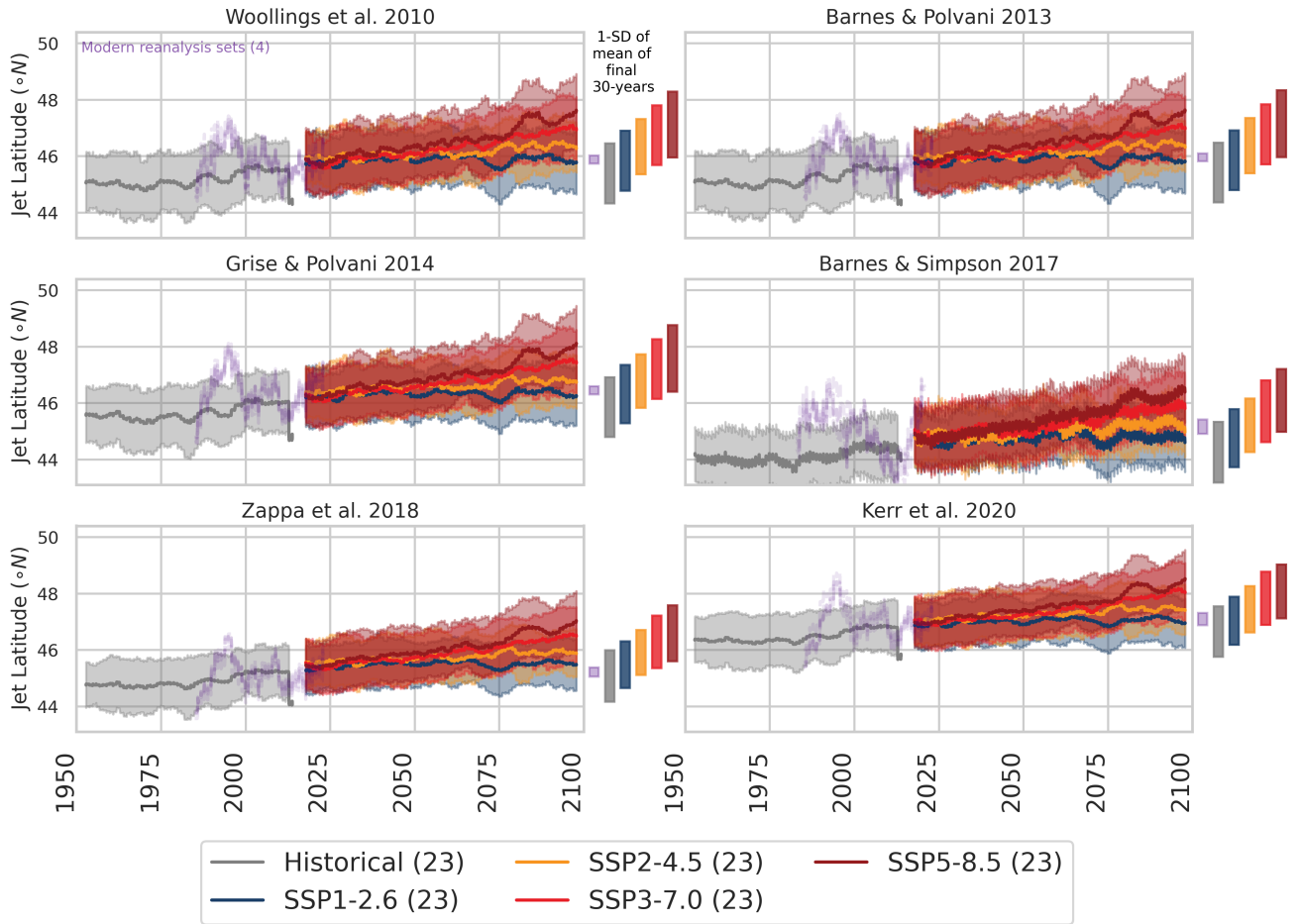


Figure S4. As for Figure 3, but for Autumn (SON).

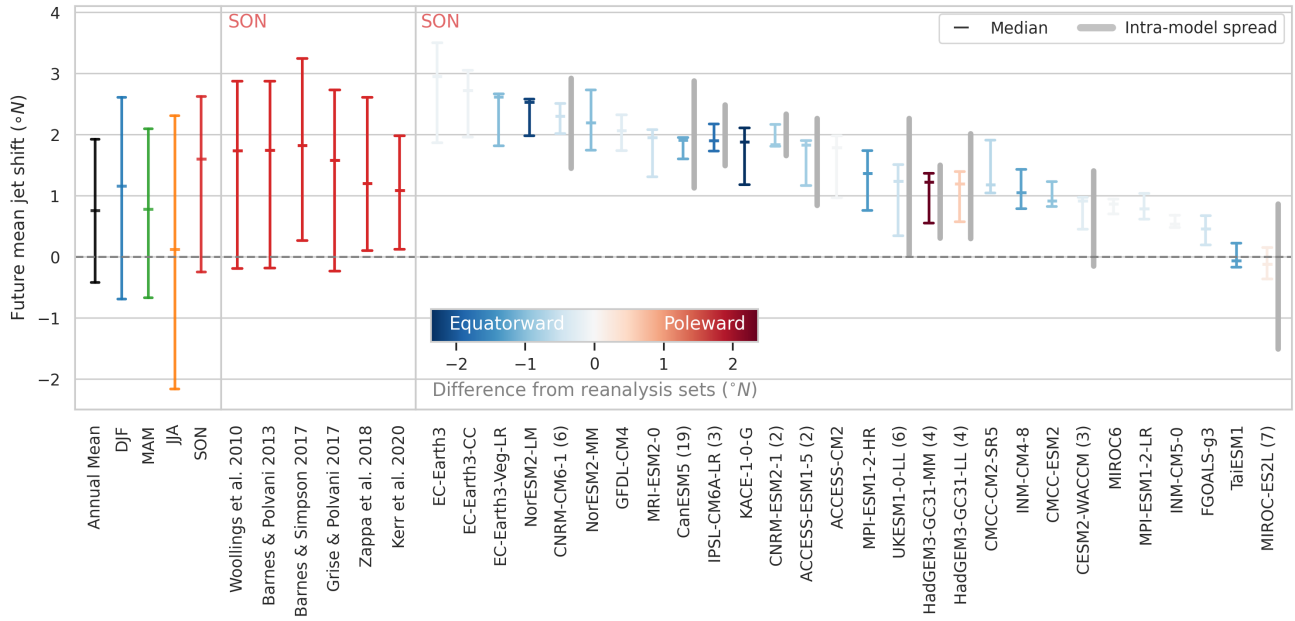


Figure S5. As for Figure 4a, but for Autumn (SON).

Table S1. Models and modelling centres of CMIP6 simulations used are listed in the first two columns. The number of realisations from the historical, SSP1-2.6, SSP2-4.5, SSP3-7.0, SSP5-8.5 experiments are shown in the remaining columns. See <https://www.ametsoc.org/PubsAcronymList> for expansions of modelling centre and model name

acronyms.

Model name	Modelling centre	historical	SSP1-2.6	SSP2-4.5	SSP3-7.0	SSP5-8.5
ACCESS-CM2	CSIRO-ARCCSS	1	1	1	1	1
ACCESS-ESM1-5	CSIRO-ARCCSS	2	2	2	2	2
CanESM5	CCCma	19	19	19	19	19
CESM2-WACCM	NCAR	3	1	1	1	4
CMCC-CM2-SR5	CMCC	1	1	1	1	1
CMCC-ESM2	CMCC	1	1	1	1	1
CNRM-CM6-1	CNRM-CERFACS	6	6	6	6	6
CNRM-ESM2-1	CNRM-CERFACS	2	2	2	2	2
EC-Earth3	EC-Earth-Consortium	1	1	1	1	1
EC-Earth3-CC	EC-Earth-Consortium	1	0	0	0	1
EC-Earth3-Veg	EC-Earth-Consortium	1	1	1	1	1
FGOALS-g3	CAS	1	1	1	1	1
GFDL-CM4	NOAA-GFDL	1	0	0	0	1
HadGEM3-GC31-LL	MOHC	4	0	0	0	4
HadGEM3-GC31-MM	MOHC	4	0	0	0	4
INM-CM4-8	INM	1	1	1	1	1
INM-CM5-0	INM	1	1	1	1	1
IPSL-CM6A-LR	IPSL	3	3	3	3	3
KACE-1-0-G	NIMS-KMA	1	1	1	1	1
MIROC-ES2L	MIROC	7	0	0	0	7
MIROC6	MIROC	1	1	1	1	1
MPI-ESM1-2-HR	DKRZ	1	1	1	1	1
MPI-ESM1-2-LR	MPI-M	1	1	1	1	1
MRI-ESM2-0	MRI	1	1	1	1	1
NorESM2-LM	NCC	1	1	1	1	1
NorESM2-MM	NCC	1	1	1	1	1
TaiESM1	AS-RCEC	1	1	1	1	1
UKESM1-0-LL	MOHC	6	6	6	6	6

Table S1